

High-temperature evolution of coercivity in nanocrystalline alloysV. Franco,^{1,2} L. F. Kiss,² T. Kemény,² I. Vincze,² C. F. Conde,¹ and A. Conde¹¹*Departamento Física de la Materia Condensada, ICMSE-CSIC, Universidad de Sevilla, P.O. Box 1065, 41080-Sevilla, Spain*²*Research Institute for Solid State Physics and Optics, Hungarian Academy of Sciences, P.O. Box 49, H-1525 Budapest, Hungary*

(Received 31 July 2002; published 23 December 2002)

The temperature evolution of the coercivity of a Finemet-type alloy, in which 10 at. % Fe has been substituted by Cr and annealed at different temperatures, has been studied. In the temperature region above the coercivity maximum, the experimental hysteresis loops have been successfully fitted by a combination of two models which use effective field controlled memory effects and temperature rescaling to describe dipolarly interacting superparamagnetic particles. It is shown that the characteristic parameters of these two models (interaction temperature and interaction field) are interrelated. A consistent two-step fitting procedure was developed which yielded physically meaningful values for the temperature dependence of the magnetic moment of the particles.

DOI: 10.1103/PhysRevB.66.224418

PACS number(s): 75.20.-g, 75.50.Tt

I. INTRODUCTION

The interactions in magnetic nanoscale granular systems have been intensively studied since more than a decade.¹ Recently, a phenomenological mean-field model was published² in order to explain the magnetic hysteresis observed in granular Cu-Co alloys well above the superparamagnetic blocking temperature of the particles. The hysteresis loops of the alloys were satisfactorily described by adding a memory term to the argument of the Langevin function used for the description of the magnetization of the non-interacting particle system. This memory term being responsible for the observed hysteresis was related to dipolar interactions between the nanometric particles, characterized by a unique adjustable parameter called effective interaction field (H_0).

The temperature dependence of the anhysteretic magnetization curves (half sum of the two branches of the hysteresis loop) was described quantitatively for the same alloys using a similar mean-field approximation.³ In this case the temperature in the argument of the Langevin function was modified with an excess temperature term (T^*) related directly to the dipolar energy between the particles. The dipolar field exerts a disordering, random torque on any magnetic moment, opposing the ordering effect of the external magnetic field. Therefore, the role of the dipolar field is similar to that of the temperature, which justifies the use of the excess temperature term in the description. As a consequence of the dipole-dipole interactions, a lower apparent moment results with respect to the interaction-free case.⁴ A roughly constant interaction temperature T^* (influenced by the temperature dependence of the saturation magnetization only) was obtained from the model, indicating that the dipolar interactions remain almost constant in the investigated temperature range. This is not surprising since the Curie temperatures of the Cu-Co alloys are much higher than the measuring temperatures used (5–700 K).

In order to study the correlation between the two interaction parameters introduced above (H_0 and T^*), the Cu-Co alloy system does not represent the best model material. The interactions between the nanoparticles can only be altered in

this system by changing the size of the particles with the use of different annealing procedures and finer variations in the strength of the interactions as a function of the measuring temperature cannot be established.

The model outlined above should be applicable to any assembly of superparamagnetic particles interacting via dipolar forces, including nanocrystalline ribbons produced by partial crystallization from an amorphous precursor. These alloys consist of two phases: ferromagnetic crystalline particles of the size of 10 nm with a Curie point of about 800 K, embedded in a ferromagnetic amorphous matrix with a varying Curie temperature up to about 600 K depending strongly on composition. If the Curie temperature of the matrix is reduced to around room temperature by properly choosing the composition and annealing, the system should behave above room temperature as an assembly of interacting nanoparticles separated by a nonmagnetic matrix. Since in this case the Curie temperature of the nanoparticles is much lower than that of the Cu-Co alloys, a much stronger change of the interactions with increasing temperature is expected.

According to the above requirements, we have studied Cr-doped FINEMET-type alloy ($\text{Fe}_{63.5}\text{Cr}_{10}\text{Nb}_3\text{Si}_{13.5}\text{B}_9\text{Cu}_1$) annealed for 1 h at different temperatures (800–825 K) to reduce the Curie point of the amorphous matrix to the vicinity of room temperature and to change systematically the particle size (10–15 nm). It was demonstrated recently^{5,6} that the hysteresis loop of one of these samples follows fairly well the theoretical predictions of the model of Allia *et al.*² In the following we will show that the temperature-dependent hysteresis loops of these alloys can only be satisfactorily described if a relationship between H_0 and T^* is assumed in the investigated temperature range (300–650 K). This modification extends the validity of the model^{2,3} for granular systems where the dipolar interactions between the particles depend strongly on temperature.

The structure of the paper will be as follows: after description of the experimental details (Sec. II) the results (Sec. III) are presented in two subsections. The microstructure of the samples used in this study is characterized in Sec. III A while the dependence of the hysteresis loops on the crystalline volume fraction and temperature is shown in Sec. III B.

The experimental results are analyzed in Sec. IV. on the base of the existing models: the hysteresis loops measured at different temperatures are fitted in Sec. IV A giving *apparent* magnetic parameters (moment and number of magnetic clusters). The temperature dependence of these magnetic parameters deduced from fitting the anhysteretic magnetization curves is discussed in Sec. IV B. Section V introduces the assumed relationship between the two interaction parameters (H_0 and T^*). It makes possible to calculate the thermal dependence of the *actual* magnetic parameters. In the last paragraph of Sec. V the problem of using a one-step procedure for obtaining the actual magnetic parameters instead of the two-step procedure used above is discussed. Conclusions are followed in Sec. VI. The possible influence of the demagnetizing field of the samples is considered in the Appendix, showing that it cannot be responsible for the observed behavior.

II. EXPERIMENTAL

Amorphous ribbon 1 cm wide and 25 μm thick of nominal composition $\text{Fe}_{63.5}\text{Cr}_{10}\text{Nb}_3\text{Si}_{13.5}\text{B}_9\text{Cu}_1$ was prepared by single roller melt spinning. The devitrification process was studied by Perkin-Elmer DSC-7 differential scanning calorimeter. Samples were annealed in halogen lamp furnace under argon stream. The crystalline volume fraction of the samples was calculated by fitting the profile of the main x-ray diffraction peak by the superposition of two pseudo-Voigt functions. The thermal dependence of the hysteresis loops has been measured by SQUID magnetometer (Quantum Design MPMS-5S) from 100 up to 700 K.

III. RESULTS

A. Microstructural characterization

The influence of the partial substitution of Fe by Cr on the microstructure of Finemet type alloys have been extensively studied in previous works.⁷ Devitrification takes place in two main stages. The first one corresponds to the appearance of (Fe,Si) nanocrystals, which remain embedded in the remaining amorphous matrix while the second one results in the appearance of boride-type phases and recrystallization phenomena. Cr addition enhances the crystallization temperature of the amorphous alloy. The peak temperature of the first crystallization exotherm increases at a rate of ~ 5 K/at.% Cr. However, no regular behavior has been found for the second crystallization process. X-ray diffraction and Mössbauer spectroscopy have also shown that there is no detectable amount of Cr in the nanocrystals, therefore, it remains in the amorphous matrix during the first crystallization stage. At the final crystallization process, Cr is incorporated into the boride type phases. Previous transmission electron microscopy studies indicate that there is a slight reduction of the (Fe,Si) crystal size as the Cr content in the precursor alloy is increased.⁸ In the present study for the three samples annealed at 800, 820, and 825 K for 1 h, a nanocrystalline volume fraction of 7, 16, and 20% with the corresponding particle size of 9, 11, and 12 nm was obtained by x-ray diffraction, respectively, which was also confirmed by TEM investigations.^{5,8}

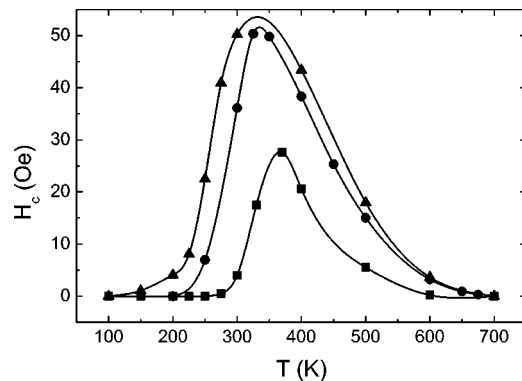


FIG. 1. Temperature dependence of coercivity for the samples with a crystalline volume fraction of 7% (squares), 16% (circles), and 20% (triangles). Lines are a guide to the eye.

B. Hysteresis loops: dependence on crystalline volume fraction and temperature

From the magnetic point of view, Cr addition reduces the Curie temperature (T_c) of the amorphous precursor, as well as that of the remaining amorphous matrix.⁹ As the first crystallization process takes place, the previously mentioned Cr enrichment of the matrix causes the progressive decrease of its Curie temperature, reaching values below room temperature.⁵ It prevents the exchange coupling of the nanocrystals via the residual amorphous matrix at room temperature.

Previous studies^{5,9} indicate that room temperature coercivity shows a different behavior than that of the Cr-free Finemet-type alloys as a function of crystalline volume fraction. Annealing at temperatures below the onset of nanocrystallization, coercivity decreases due to stress relaxation. At the beginning of nanocrystallization, coercivity increases due to the appearance of the magnetocrystalline anisotropy of the (Fe,Si) grains, but in contrast to the usual Finemet behavior, the further increase of the crystalline volume fraction does not reduce coercivity. This was explained by the reduced coupling between the grains due to the paramagnetic character of the matrix at this temperature.

Figure 1 shows the thermal dependence of coercivity for three samples with different crystalline volume fractions (7, 16, and 20%) determined from the measured temperature-dependent hysteresis loops, an example of which is seen in Fig. 2. For all of them, three different temperature regimes can be distinguished. For low temperatures, the reduced values of coercivity are explained by the random anisotropy model extended to two-phase systems:¹⁰ the magnetization of the nanocrystals—which are coupled through the ferromagnetic amorphous matrix—cannot follow the local easy axes and the magnetocrystalline anisotropy is averaged out. As the matrix becomes paramagnetic, it can no longer exert this influence and coercivity progressively increases.¹¹ The final temperature regime, which corresponds to the decrease of coercivity at higher temperatures, is ascribed to the transition from slightly coupled particles to the superparamagnetic regime.

Figure 1 hints at a progressive decrease of the temperature of the coercivity maximum with increasing crystalline vol-

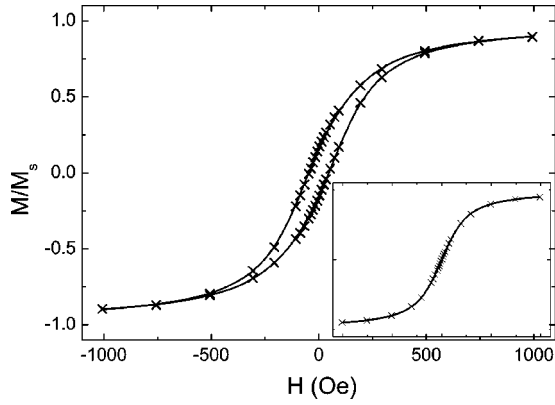


FIG. 2. Experimental (crosses) and modeled (line) hysteresis loop of the sample with 20% crystalline volume fraction measured at 400 K. Inset: Langevin fitting of the anhysteretic curve.

ume fraction. It seems to be in contradiction with the behavior observed for the Cr-free Finemet-type alloys,¹¹ where the opposite trend is observed. However, in the latter case the Curie temperature of the residual amorphous phase increases with the crystalline volume fraction whereas T_c of the residual amorphous phase for the Cr-doped Finemet-type alloys decreases (as evidenced by the decreasing temperature vs crystalline volume fraction, at which coercivity begins to increase, as well as from previously reported results⁵). Therefore, the difference between the peak temperature of H_c and the Curie temperature of the residual amorphous phase increases with the crystalline volume fraction, in agreement with the behavior found for Cr-free Finemet type alloys.

IV. ANALYSIS OF THE RESULTS

A mean-field model for describing the hysteresis loops of dipolarly interacting superparamagnetic particles was originally applied to Cu-Co granular magnetic systems.² It should be able to reproduce the magnetic hysteresis of any granular system with dipolarly interacting superparamagnetic particles embedded in a nonmagnetic matrix. Therefore, this model was applied to a nanocrystalline Cr-containing Finemet-type alloy at room temperature.⁵ In the following, the temperature dependence of the hysteresis loops above the temperature of the maximum H_c in Fig. 1 will be analyzed for different crystalline volume fractions.

A. Hysteresis loop model

The mean field model considers the effect of the dipolar interactions between the particles as a memory function. Taking into account that the noninteracting particles should behave as a superparamagnet, it is logical to assume that the skeleton of the loop should correspond to a Langevin function. (As the extension to a distribution of particle sizes is straightforward and not necessary for the case discussed here, it will not be considered in this paper.) Defining the memory function $\delta(m, m_v)$, as depending on the reduced magnetization of the sample m , and the maximum achieved magnetization in the loop m_v (vertex magnetization), the branches of the loop can be described as

$$m_{\pm} \approx L \left(\frac{\mu H}{kT} \pm \delta(m, m_v) \right), \quad (1)$$

where μ is the magnetic moment of the particle (which will be referred later as the apparent magnetic moment), H is the applied field, T is the measuring temperature, and k is Boltzmann's constant.

The effect of dipolar interaction can be expressed in the form of a mean field H_{mean} :

$$m_{\pm} = L \left(\frac{\mu}{kT} (H \pm H_{\text{mean}}) \right), \quad (2)$$

where $\delta(m, m_v) = (\mu/kT)H_{\text{mean}}$. The mean field, H_{mean} can be rewritten as a function of an effective interaction field H_0 (related to the root-mean-square of the dipolar field) and a "cutoff" function $F(m)$ as follows:

$$H_{\text{mean}} = H_0 [F(m) - F(m_v)]. \quad (3)$$

To be able to reproduce the hysteresis loops of dipolarly interacting particles, the memory function should produce closed hysteresis loops. Also, as the interactions are irrelevant at saturation, the memory function must have a larger effect when the magnetization change is larger and should be an even function of the reduced magnetization. It can be checked that an expression such as Eq. (3), imposing that $F(m)$ should have a value equal to 1 for zero magnetization value, and zero value at saturation, fulfils all the required conditions.²

It is also known² that the half sum of the two branches of the hysteresis loop (anhysteretic curve in the following) reduces to a Langevin function in the case when the particles interact through a dipolar field. Therefore, the magnetic moment of the particles can be calculated through a simple Langevin fitting of the anhysteretic curve. On the other hand, the reduced half difference of the two branches [$\Delta(m)$] is a measure of how the hysteresis loop separates from the superparamagnetic skeleton. Therefore, it should be related to the cutoff function. Defining m_R as the reduced remanence of a major loop (which will only be considered), the cutoff function can be obtained as

$$F(m) = \frac{\Delta(m)}{3 m_R L'(m)}, \quad (4)$$

where $L'(m)$ is the first derivative of the Langevin function with respect to its argument. The different parameters required for reconstructing the branches of a major loop are obtained as follows. The magnetic moment is determined from the Langevin fitting of the anhysteretic curve; the cutoff function is obtained from the reduced half difference of the branches through Eq. (4) and finally, the interaction field is calculated from

$$m_R = \frac{1}{3} \frac{\mu H_0}{kT}. \quad (5)$$

The major loop is obtained as

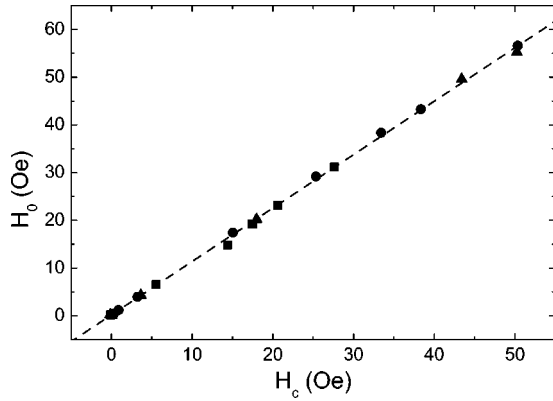


FIG. 3. Relationship between the interaction field and coercivity of all the three studied samples (squares: 7%; circles: 16%; triangles: 20% crystalline volume fraction) measured at different temperatures above the coercivity maximum.

$$m_{\pm} = L \left(\frac{\mu H}{kT} \pm \frac{\mu H_0}{kT} F(m) \right). \quad (6)$$

Following this procedure, the hysteresis loops of the different nanocrystalline samples can be modelled with remarkable agreement above the temperature range starting from the coercivity maximum. As an example, Fig. 2 shows the experimental (crosses) and calculated loop of the sample with 20% crystalline volume fraction measured at 400 K. The inset corresponds to the Langevin fitting of the anhysteretic curve.

B. Thermal dependence of magnetic parameters

When the previously described procedure is applied to the studied samples measured at different temperatures, the thermal evolution of the characteristic parameters can be studied for different crystalline volume fractions. The effective interaction field has a temperature dependence which is similar to that measured for coercivity. Figure 3 shows the linear correlation between these two quantities when the data for all the samples are plotted, the hidden variable is the temperature. This behavior is consistent with the assumption that the most important interaction between the particles is of dipolar origin.

When the temperature dependence of the magnetic moment is studied (Fig. 4), an increase of this parameter with increasing temperature is clearly observed in all cases. Although this effect could indicate structural evolution of the samples during the measuring process (giving rise to an increasing crystal size), this has been ruled out by checking the reversibility of this thermal dependence. Therefore, the calculated magnetic moment is an effective one and the magnetic moment and the number of particles will be denoted as “apparent” parameters in the following, due to the fact that their thermal evolution is not related with the intrinsic characteristics of the nanocrystals. In principle, the increasing value of the apparent magnetic moment for increasing temperature can be also influenced by the demagnetizing field of

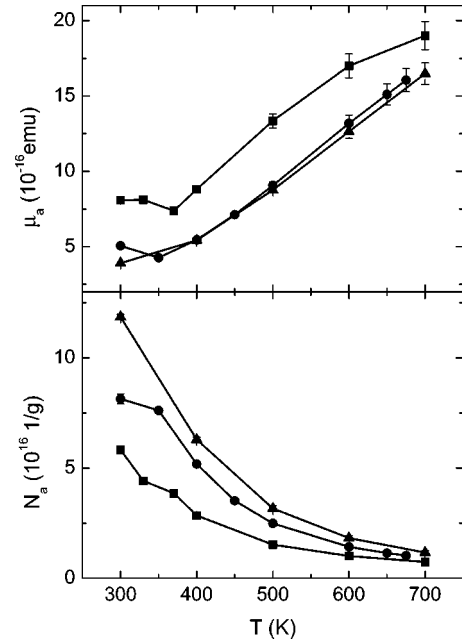


FIG. 4. Temperature dependence of the apparent magnetic moment and the number of particles per unit mass, obtained from the Langevin fitting of the anhysteretic magnetization curves (symbols as in Fig. 1).

the sample. It can be shown (see the Appendix) that this effect cannot be the dominant contribution to the temperature dependence of the moment.

Recently, Allia and co-workers have presented an extension of the model that reproduces the thermal dependence of the anhysteretic magnetization curve of Cu-Co nanocrystalline alloys.³ This model should be able to describe the temperature evolution of the apparent magnetic moment of the dipolarly interacting superparamagnetic (Fe,Si) particles present in the Cr-containing Finemet-type alloys.

In this model³ the classical Langevin description is extended by an effective interaction temperature (T^*) term added to the measuring temperature. This new term is expected to take into account the disordering effect of the dipolar interactions between the particles. Although T^* makes the magnetization have a functional form which resembles that of a Curie-Weiss approach, it has to be noted that T^* is a temperature dependent parameter, as will be shown below.

The anhysteretic curve can be described either by the apparent parameters

$$M = N_{\text{app}} \mu_{\text{app}} L \left(\frac{\mu_{\text{app}} H}{kT} \right), \quad (7)$$

or by the “actual parameters” (those emerging from the intrinsic characteristics of the nanoparticles) together with the interaction temperature

$$M = N \mu L \left(\frac{\mu H}{k(T+T^*)} \right). \quad (8)$$

As both are descriptions of the same experimental data, both should give the same values for the saturation magne-

tization and the initial susceptibility. This requirement gives the relationship between apparent and actual parameters

$$\mu_{\text{app}} = \frac{1}{1 + T^*/T} \mu, \quad (9)$$

$$N_{\text{app}} = (1 + T^*/T)N. \quad (10)$$

According to Allia *et al.*,³ the interaction temperature, T^* is related to the dipolar energy through the relation $kT^* = \alpha\mu^2/d^3$, where d is the interparticle distance and α is a temperature-independent proportionality constant which cannot be obtained from first principles, as it depends on the geometrical distribution of the particles, correlations between adjacent moments, etc. Taking Eq. (8) for small fields, it can be easily shown that the applicability of the model can be checked by looking for a linear relationship between the reciprocal initial susceptibility of the anhysteretic curve and T/M_s^2 . However, in our case for the Cr-containing Finemet type alloys, such a linearity is not found. This can be due to a temperature dependent α , whose evolution is not due to modifications of the microstructure but to the effect of magnetic relaxation of the nanoparticles as the interaction field is reduced to zero. This temperature dependence is not taken into account in the original model,³ which can explain the failure when it is applied in a temperature range which approaches the pure superparamagnetic regime (negligible interparticle interactions).

V. RELATIONSHIP BETWEEN THE INTERACTION PARAMETERS

Both approaches of Allia *et al.*^{2,3} are independent models for representing the same physical system: an ensemble of dipolarly interacting superparamagnetic particles. In the first model,² the interactions are considered as the origin of the experimentally observed hysteresis loops and they are modeled by introducing an interaction field which is related to the r.m.s. dipolar field. The second model³ reproduces the decrease of the apparent magnetic moment of the particles through an effective interaction temperature which is connected with the r.m.s. dipolar energy. When the temperature dependence of T^* is determined by that of μ through the above postulated relation $T^* \approx \mu^2$, both models are able to reproduce the overall behavior of the Cu-Co granular magnetic systems. However, for Cr-containing Finemet-type alloys, that particular temperature dependence of T^* seems not to be valid. The main difference of the two systems is the Curie temperature of the nanocrystals. While for the Cu-Co alloys the particles are Co nanocrystals, with a T_c much higher than the temperature range where the loops are studied (increasing this range would result in the undesirable effect of structural evolution of the samples during the measurements), in the case of Cr-Finemet, the (Fe,Si) nanocrystals have a much lower T_c . For the Cu-Co alloys, simple superparamagnetic behavior is not found in the studied temperature range,³ but for Cr-Finemet it is possible to reach zero coercivity (Fig. 1). As the interactions between the particles depend on their saturation magnetization (as well as on

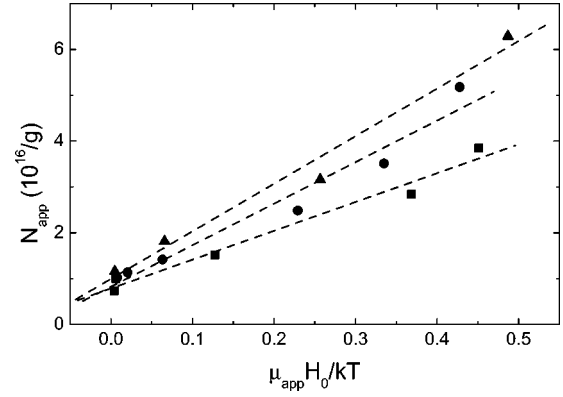


FIG. 5. Linear dependence of the apparent number of particles per unit mass with the ratio of the magnetic interaction energy to the thermal energy. The linear behavior confirms the proportionality between the effective energy giving rise to the observed coercivity ($\mu_{\text{app}} H_0$) and the effective interaction thermal energy kT^* . The presented points are for temperatures above the coercivity maximum (symbols as in Fig. 1). Broken lines are linear fits to the data points.

geometrical considerations), for the Cr-Finemet the strength of the dipolar interaction covers a broader range.

Therefore, it is logical to assume that the parameters of the previous models^{2,3} (the interaction field H_0 and the effective temperature T^* , respectively) are interrelated. The simplest relationship between the parameters would be to consider that the thermal energy of the interactions (kT^*) is proportional to the energy term giving rise to the coercivity of the loops ($\mu_{\text{app}} H_0$)

$$kT^* = \xi \mu_{\text{app}} H_0. \quad (11)$$

Note that in Eq. (6) the moment corresponds to that directly obtained from the Langevin fitting of the anhysteretic curves, which was subsequently denoted as *apparent*.

By using this proportionality assumption in Eq. (10) and taking into account that there is no structural evolution in the samples for the different measuring temperatures (N should remain temperature independent and characteristic for each of the samples), N_{app} should be linearly dependent on $(\mu_{\text{app}} H_0)/(kT)$. Figure 5 shows the linear dependence of the parameters obtained from the experimental hysteresis loops in the temperature range where dipolar interactions should be predominant (temperatures above the coercivity maximum). The actual number of particles per unit mass are determined from the axial intercept of the line and it coincides with the high temperature limit of N_{app} (interaction free region). It should be mentioned, however, that there is a tendency of the points corresponding to high N_{app} to deviate from a linear behavior. It also seems that this curvature is larger for the higher crystalline volume fractions. Therefore, it could be related to the fact that at these lower temperatures interactions are probably not purely dipolar.

As an internal check of this modified model, Fig. 6 plots the values of the apparent magnetic moment directly calculated from the experimental data and those obtained from Eq.

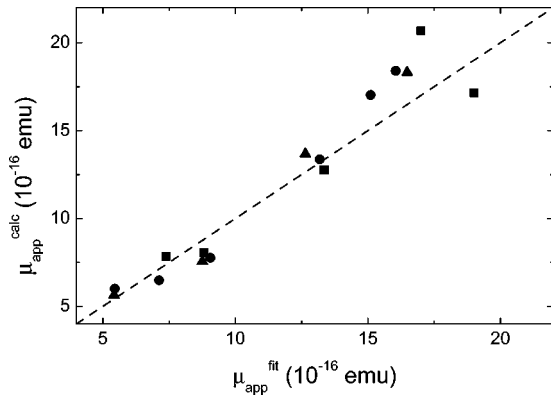


FIG. 6. Correlation between the apparent magnetic moment calculated from the Langevin fitting of the anhysteretic curves and the same parameter predicted by the model, using Eqs. (9) and (11) (symbols as in Fig. 1). Line corresponds to slope 1.

(9), using the effective temperature T^* . The linear behavior with a slope close to 1 and an intercept close to zero shows the adequacy of the model.

Figure 7 shows the temperature dependence of the magnetic moment of the particles μ as deduced with our assumption. As discussed formerly, simple Langevin fitting with the apparent parameters [Eq. (7)] would indicate that the particle size decreases with increasing annealing temperature. This would be in contradiction with TEM observations.⁸ The presented analysis [a combination of the two models of Allia *et al.*^{2,3} using Eq. (11) as a proportionality law] corrects this tendency, giving larger magnetic moments for the samples annealed at higher temperatures. The similarity of the magnetic moment values of the samples with 16 and 20% crystalline volume fractions is in agreement with the crystal sizes obtained from x-ray diffraction, which indicates that grain size saturates to a value close to 12 nm. An estimated error bar for the calculated actual moments is indicated, showing that it is comparable with the crossing of the two curves of the lowest crystalline volume fraction sample at high tem-

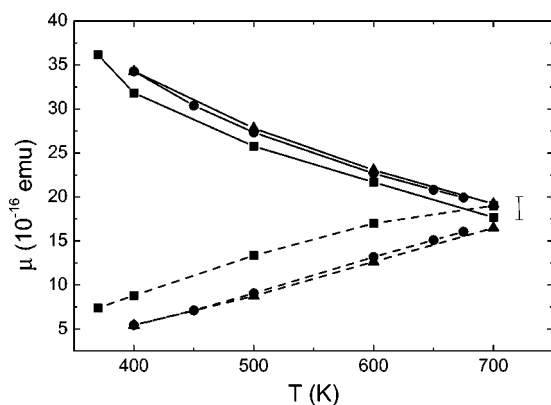


FIG. 7. Temperature dependence of the apparent (dashed line) and actual (solid line) magnetic moment of the three studied samples: squares: 7%; circles: 16%; triangles: 20% crystalline volume fraction. The estimated error bar for the actual moment is given, being of the same size of the crossing of the two curves for the lowest crystalline volume fraction.

peratures. The figure also shows that the actual magnetic moment of the particles decreases with increasing temperature, as expected when no structural evolution occurs in the measuring temperature range. It has to be mentioned, however, that the moments of the samples at temperatures near the coercivity maximum can be overestimated, as for this region the contribution of other types of interactions might have an influence on the results. The concave shape of the magnetization curve is a feature also observed for Cu-Co alloys³ and can be related to a gradual transition of some of the particles to simple superparamagnetic regime; a more detailed study of this feature is planned.

The physical reason for the proportionality of T^* and $\mu_{\text{app}} H_0$ might be the following: the approach proposed by Allia *et al.* is based on the temperature independence of α , which should be true for low temperatures (well below the Curie temperature of the nanoparticles), as their geometrical distribution, and correlations between neighboring particles remain constant. However, it can be expected that with increasing temperature, the changing magnetic moment of the particles can alter the correlations between neighboring particles. This can produce a temperature evolution of α , which cannot be accounted for in the approach of Allia *et al.*³ but it is incorporated into the temperature evolution of the mean field energy term $\mu_{\text{app}} H_0$ obtained from the fittings. Moreover, as the temperature is increased, the thermal energy gains importance over the interaction energy. Therefore, the essential difference between both approaches is that, in the former, the thermal dependence is imposed into the formulation, while in the present approach the thermal dependence of the interactions is obtained from the experimental hysteresis loops through the energy term $\mu_{\text{app}} H_0$.

Using the present approach, the actual magnetic moment of the samples can be obtained in a two-step procedure. First, the interaction field is calculated together with the *apparent* magnetic parameters and second, the *actual* magnetic parameters are obtained via these data. A closed description of the problem would be desirable by fitting simultaneously the interaction field, the effective temperature and the actual magnetic parameters. For this purpose, T^* should be introduced inside the argument of the Langevin function from the beginning and the anhysteretic curves should be fitted to Eq. (8). Using this approach, only the ratio $\mu/(T+T^*)$ can be calculated. To separate the interaction temperature it would be necessary to introduce some estimations of the magnetic moment, obtained from the grain sizes observed by TEM or XRD. This would also make the procedure a two-step process, with the drawback of having to impose a certain relationship between grain size and effective magnetic moment, which can be cumbersome in some cases.

VI. CONCLUSIONS

It was established in this work that Cr doped FINEMET-type alloy is a highly attractive model material to study the magnetic interactions in nanoscale granular systems, as all the characteristic temperature ranges of qualitatively different magnetic behaviors are experimentally accessible. The good soft magnetic behavior at low temperatures is followed

by an intensive maximum of the coercive field, which decreases to zero as expected for superparamagnetic particles when the interaction energy is much smaller than the thermal energy. The hysteresis loop models of Allia *et al.*^{2,3} based on the dipolar interaction among magnetic nanoparticles have been found to be applicable above the temperature of the coercive field maximum. As it was shown that no further structural changes occur in the temperature range where the coercive field decreases from its maximum value to zero, this system is a more severe testing ground for the model than the Cu-Co system it was originally developed for.

These advantageous features of the Cr doped FINEMET-type alloy make it possible to establish the connection between the parameters used in the different versions of the dipolar coupling models. It was established that the effective energy giving rise to the observed coercivity ($\mu_{\text{app}} H_0$) and the effective interaction thermal energy, kT^* should be proportional and this assumption made it possible to develop a consistent two-step fitting procedure, which yielded physically reasonable values. In this frame, first an apparent effective moment, apparent number of particles and interaction field are fitted to the measured hysteretic curves. In the second step, the apparent parameters are rescaled by the interaction temperature, which is fitted to the temperature dependence of the anhysteretic curves. The consistency of the numerical procedure was checked by studying the temperature dependence and particle size effects influenced by different degree of nanocrystallization. It has been verified that in contrast to the apparent moment, the rescaled moment increases with the nanocrystalline fraction (where TEM results in fact find the increase of the grain size) and the physically expected temperature decrease of the magnetic moments has also been found. The simultaneous fitting of all the parameters, on the other hand, has been proven not to be feasible.

ACKNOWLEDGMENTS

This work was supported in part by the Spanish Ministry of Science and Technology and E.U.-FEDER (Project No. MAT2001-3175), the PAI of Junta de Andalucía, the Hungarian Research Fund (Grant Nos. OTKA T-030753 and T-038383) and the Hispano-Hungarian Bilateral Cooperation Program (Grant No. TET E-2/2001). V.F. is grateful to the CMRC (Condensed Matter Research Center) for supporting his stay in Budapest in the program WP9.

APPENDIX

The increasing value of the apparent magnetic moment for increasing temperature can be influenced by the demag-

netizing field of the sample. In this appendix, it will be checked by simple calculations whether this contribution can be relevant. Let us assume that the demagnetizing field of the sample is responsible for the temperature dependence of the apparent magnetic moment. The relationship between the apparent and intrinsic susceptibility of a sample is given by

$$\chi_{\text{app}} = \frac{\chi}{1 + N_d \chi}, \quad (\text{A1})$$

where N_d is the demagnetizing factor. In our case, the initial susceptibility of the alloy can be obtained from the power expansion of the Langevin function, therefore

$$\chi_{\text{app}} = \frac{N_{\text{app}} \mu_{\text{app}}^2}{3kT}, \quad (\text{A2})$$

$$\chi = \frac{N \mu^2}{3kT}. \quad (\text{A3})$$

By substituting these expressions into Eq. (A1) and taking into account that the value of saturation magnetization should be the same in both descriptions ($M_s = N \mu = N_{\text{app}} \mu_{\text{app}}$), a relationship between the apparent and actual magnetic moment can be obtained:

$$\mu_{\text{app}} = \frac{\mu}{1 + N_d M_s \mu / 3kT}. \quad (\text{A4})$$

By identifying terms in this equation with those of Eq. (9), the interaction temperature can be rewritten as

$$T^* = \frac{N_d M_s \mu}{3k}. \quad (\text{A5})$$

Considering that the demagnetizing factor of the samples (~ 2 mm long and ~ 25 μm thick) is of the order of 10^{-2} , and using the typical values of the parameters for the sample with the highest crystalline volume fraction at ~ 400 K ($\sigma_s \sim 35$ emu/g, $\mu \sim 30 \times 10^{-16}$ emu, $\rho \sim 8$ g/cm³ and $\xi/k \sim 50$ K/G), the resulting interaction temperature would correspond to ~ 20 K, which should produce a coercivity of ~ 0.4 Oe [Eq. (11)]. This value is two orders of magnitude smaller than the measured coercivity.

In conclusion, although the demagnetizing field can have some effect on the temperature dependence of the apparent moment, it cannot be the dominant contribution to this effect. The exact calculation of the demagnetizing field, however, is a cumbersome issue, as not only the external shape of the sample has to be taken into account, but also the contribution of each particle, which are embedded in a paramagnetic matrix. It is out of the scope of the present analysis.

¹J. Dormann, D. Fiorani, and E. Tronc, *Adv. Chem. Phys.* **98**, 283 (1997).

²P. Allia, M. Coisson, M. Knobel, P. Tiberto, and F. Vinai, *Phys. Rev. B* **60**, 12 207 (1999).

³P. Allia, M. Coisson, P. Tiberto, F. Vinai, M. Knobel, M. Novak, and W. Nunes, *Phys. Rev. B* **64**, 144420 (2001).

⁴D. Kechrakos and K. Trohidou, *Phys. Rev. B* **62**, 3941 (2000).

⁵V. Franco, C.F. Conde, A. Conde, L.F. Kiss, D. Kaptás, T. Ke-

- mény, and I. Vincze, *J. Appl. Phys.* **90**, 1558 (2001).
- ⁶V. Franco, C. F. Conde, A. Conde, L. F. Kiss, and T. Kemény, *IEEE Trans. Magn.* **38**, 3069 (2002).
- ⁷C.F. Conde, M. Millán, and A. Conde, *J. Magn. Mater.* **138**, 314 (1994).
- ⁸M. Millán, C.F. Conde, and A. Conde, *J. Mater. Sci.* **30**, 3591 (1995).
- ⁹V. Franco, C.F. Conde, and A. Conde, *J. Magn. Mater.* **203**, 60 (1999).
- ¹⁰A. Hernando, M. Vázquez, T. Kulik, and C. Prados, *Phys. Rev. B* **51**, 3581 (1995).
- ¹¹A. Hernando, P. Marín, M. Vázquez, and G. Herzer, *J. Magn. Mater.* **177-181**, 959 (1998).